# Kinetic Study on the Removal of Organic Pollutants by an Electrochemical Oxidation Process

**Anna Maria Polcaro,* Michele Mascia, Simonetta Palmas, and Annalisa Vacca**

*Dipartimento di Ingegneria Chimica e Materiali, Università degli Studi di Cagliari, Piazza d'armi, 09123 Cagliari, Italy*

This paper deals with the kinetics of electrochemical oxidation of 2,6-dichlorophenol and *p*-hydroxybenzoic acid in phosphate buffer at pH = 7. On the basis of experimental results, a mathematical model was formulated which effectively describes the trend in time of the concentration of the organic compounds involved in the electrochemical oxidation process. The proposed kinetic model is based on a reaction mechanism which takes into account both the direct oxidation of the organic substrate at the electrode surface and the indirect oxidation, in the liquid phase, by means of electrogenerated oxidizing agents. The model well interprets the complex effect on the removal efficiency of such operating parameters as the current density, the linear velocity of the electrolyte, and the ratio between the anode surface and solution volume.

## Introduction

The removal of toxic or biorefractory compounds from aqueous wastes by electrochemical oxidation is a promising treatment which may be considered a useful alternative to chemical and photochemical oxidation.

Several experimental works have appeared in the literature on electrochemical degradation processes,[1] most of which have focused on the direct anodic oxidation of synthetic solutions of model organic substances.[2−7] Particular emphasis has been placed on the study of the electrocatalytic properties of the anode material to select a suitable electrode at which effective degradation of organic compounds can be performed, up to their complete mineralization or, at least, to their conversion to biodegradable compounds. Among others, Ti/$SnO_2$ and Fe(III)-doped $\beta$-$PbO_2$ electrodeposited on Ti seemed to have high catalytic activity;[8−10] good performances have also been shown by diamond-doped-with-boron electrodes. These have recently been tested for scientific purpose but are still not in use commercially.[11,12]

Moreover, commercial electrodes with proven stability and low cost, such as Pt film electrodes or Ti/$IrO_2$ and Ti/$RuO_2$ electrodes, have been widely used to remove organic compounds from either real wastewater[13−17] or model solutions.[18,19] Although these electrodes usually show low faradaic efficiencies toward the oxidative degradation of organic compounds, good performances have been obtained when the solution contains inorganic species, in particular $Cl^-$ ions which are able to mediate the oxidation process.[20−22] The reaction path for the latter process has been examined but is not well understood; therefore, the aim of this work is to provide further information in order to explain the mechanism that occurs when organic compounds, in particular phenols, are electrochemically oxidized at these electrodes in the presence of $Cl^-$ ions. To this aim, the electrochemical oxidation of 2,6-dichlorophenol (DCP) and *p*-hydroxybenzoic acid (PHB) has been investigated by using an undivided cell and a commercial (dimensionally stable anode, DSA) anode, with a coating of $RuO_2$. The compounds have been selected because of the different nature of the substituting groups in the aromatic ring, which confers upon DCP and PHB different reactivities to oxidation.

The results from experiments performed under different conditions are presented and discussed in this paper.

## Experimental Section

Experimental runs were carried out in an undivided electrochemical flow cell, which was inserted into a hydraulic circuit: the cell consisted of a 0.4 $dm^3$ glass tank; the circuit was comprised of a 1 $dm^3$ reservoir and a centrifugal pump. The electrolyte was continuously pumped from the reservoir to the cell and back, in a closed loop; electrolyte flow rates ranged between 0.5 and 10 $cm^3\ s^{-1}$.

The electrode materials were stainless steel for the cathode and Ti/$RuO_2$ (DSA, provided by De Nora, Milan) for the anode. Two cathodes (5 × 11 $cm^2$) were placed in the cell; a grid of DSA (5 × 11 $cm^2$; void fraction 0.54) with both faces active as the anode was inserted between the cathodes with an interelectrode gap of 1 cm. A saturated calomel electrode (SCE) was used as the reference electrode.

Appropriate volumes of solution were adopted during the runs in order to achieve ratios between the anode area and solution volume ranging from 3.3 to 6.5 $m^{-1}$.

Working solutions covering a concentration range from 0.4 to 0.5 g $dm^{-3}$ were prepared by dissolving DCP and/or PHB in a 0.2 M phosphate buffer at pH = 7. To investigate the influence of chloride ions on the oxidation process, in some runs KCl was added to the solutions, up to a concentration of 1 g $dm^{-3}$ of chloride ions.

The temperature was controlled by immersing the reservoir in a thermostatic bath at 25 ± 2 °C.

During the runs, samples of electrolyte were withdrawn and analyzed for the concentration of reactant and products by high-performance liquid chromatography (HPLC) analysis (UV detector; column Chrompack Chromsphere 5 C8 ODS; mobile phase, $CH_3OH$ + 0.1% $H_3PO_4$ and 0.05 M $KH_2PO_4$ + 0.1% $H_3PO_4$; flow rate, 1.7 $cm^3\ min^{-1}$; column temperature, 25 °C). The con-

* Corresponding author. Tel.: ++390706755059. Fax: ++390706755067. E-mail: polcaro@dicm.unica.it.

10.1021/ie010669u CCC: $22.00 
Published on Web 05/17/2002

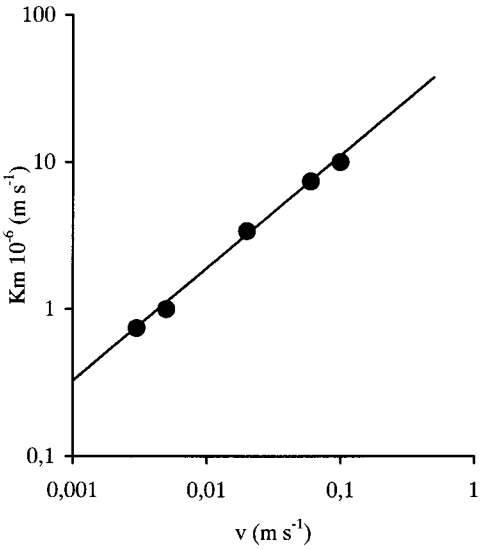


**Figure 1.** Mass-transfer coefficients as a function of the linear flow velocity.

centration of oxidizing species, mainly consisting of $HClO/ClO^-$, produced by chloride oxidation at the working pH, was also determined by the photometric method (Reflectoquant Plus Merck).

The trend of the oxidative process of the phenols was monitored by measuring the chemical oxygen demand (COD) of the samples through a Merck SQ118 instrument.

## Results

Several sets of electrolyses were performed with solutions containing phenolic compounds singly or in mixtures to evaluate the effect of the following parameters on electrochemical degradation: hydrodynamics of the cell, current density, ratio betweens the anode area and solution volume, and composition of the electrolyte.

To characterize mass transfer from the anode surface to the bulk solution, the well-established technique based on the determination of the limiting current density value ($i_{lim}$) was used.[23] The values of $i_{lim}$ were obtained for the oxidation of a 0.1 M ferrocyanide solution in an alkaline medium in the presence of 1 M $KNO_3$ as the supporting electrolyte: the flow rates ranged from 5 to 100 cm$^3$ s$^{-1}$, which corresponded to a range of linear velocity ($u$) from 0.5 to 10 cm s$^{-1}$.

Figure 1 reports the relationship between the mass-transfer coefficient ($k_m$) and the linear velocity of the electrolyte: the values of $k_m$ were calculated from the $i_{lim}$ values by the following relation:

$$i_{lim}/zF = k_m C^b \qquad (1)$$

where $C^b$ represents the concentration of the ion ferrocyanide in the bulk solution. The $\ln(k_m)$ vs $\ln(u)$ data are fitted well by a straight line, whose slope (0.8) is in agreement with the typical correlations available in the literature for mass transfer to or from plate to fluid.[24]

Another set of preliminary experiments was performed to verify the formation in a solution which did not contain phenols of strongly oxidizing compounds (OX in the rest of the text). Electrolyses of a 0.2 M phosphate solution, buffered at pH = 7, were performed in both the presence and absence of chloride ions.

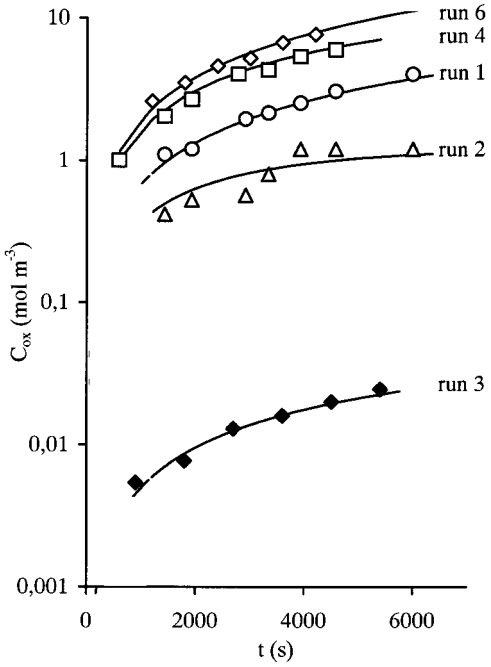


**Figure 2.** Trend in time of experimental and calculated OX concentrations during electrolysis of the supporting electrolyte in different experimental conditions. The values of the parameters used for the calculated values are reported in Table 1.

Evolution of $O_2$ and $H_2$ at the anode and cathode, respectively, always occurred during these runs; however, in all of the adopted conditions, the formation of OX was observed.

As can be noted from Figure 2 in which the concentration of such compounds is reported as a function of the electrolysis time, the higher concentration of OX is measured in solutions containing chlorides when a high current density and a low electrolyte flow rate are adopted.

The faradaic efficiency $\epsilon_F$ for the anodic generation of OX can be obtained from the following mass balance:

$$V\frac{dC_{OX}}{dt} = \epsilon_F\frac{I}{zF} - A_C k_m C_{OX} \qquad (2)$$

The second term on the right side of eq 2 takes into account the cathodic reduction of the soluble OX. In fact, because of the absence of the membrane between the anodic and cathodic compartments, the species produced at the anode can easily reach the cathode, where they are reduced under mass-transfer control.

Integration of eq 2 with the initial condition, $t = 0$ and $C_{OX} = 0$, leads to

$$C_{OX} = \epsilon_F\frac{I}{zFA_C k_m}[1 - e^{-(A_C k_m/V)t}] \qquad (3)$$

Values of $\epsilon_F$ obtained by fitting with eq 3 the experimental $C_{OX}$ vs $t$ data at different current densities and electrolyte compositions are shown in Table 1.

Finally, galvanostatic electrolyses, in which DCP and PHB were oxidized, were performed in different experimental conditions: the current density adopted in these electrolyses range from 100 to 200 A m$^{-2}$, and the anodic potential assumed values in the range of 1.2−1.4 V, depending on the experimental conditions. The results obtained in these runs are shown in Figures 3 and 4, where the fraction of removed phenol $\xi = 1 - C(t)/C(0)$

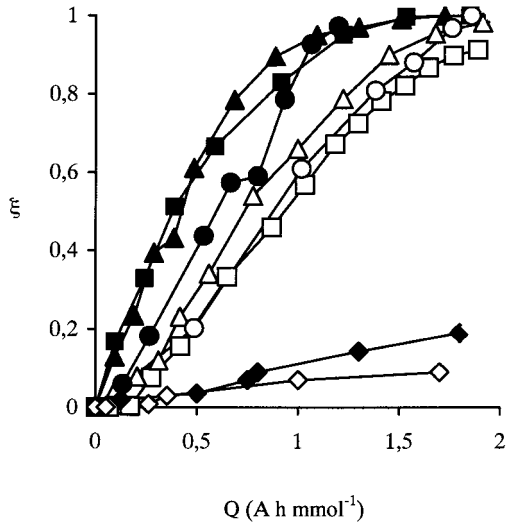


**Figure 3.** Trend of COD during electrochemical oxidation of DCP (full symbols) or PHB (empty symbols) as a function of the specific charge supplied. All of the values are obtained at $k_m = 0.97 \times 10^{-6}$ m s$^{-1}$: (△▲) $i = 200$ A m$^{-2}$, $A/V = 6.5$ m$^{-1}$, [Cl$^-$] = 1000 mg dm$^{-3}$; (□■) $i = 100$ A m$^{-2}$, $A/V = 6.5$ m$^{-1}$, [Cl$^-$] = 1000 mg dm$^{-3}$; (○●) $i = 200$ A m$^{-2}$, $A/V = 3.3$ m$^{-1}$, [Cl$^-$] = 1000 mg dm$^{-3}$; (◇◆) $i = 200$ A m$^{-2}$, $A/V = 3.3$ m$^{-1}$, [Cl$^-$] = none.

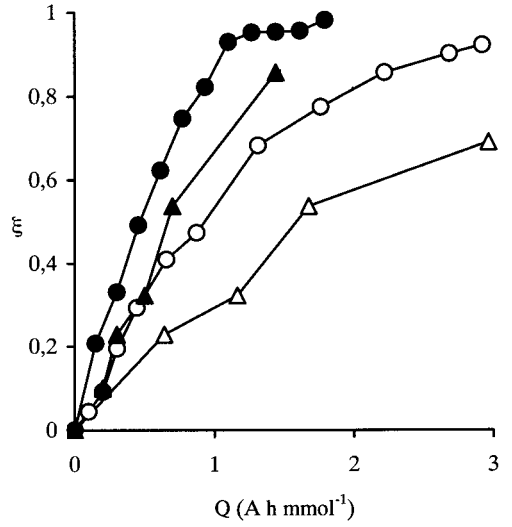


**Figure 4.** Fraction of organic removed during electrochemical oxidation of DCP (full symbols) or PHB (empty symbols) as a function of the specific charge supplied. All of the values are obtained at $k_m = 0.97 \times 10^{-6}$ m s$^{-1}$: (△◆) $i = 200$ A m$^{-2}$, $A/V = 6.5$ m$^{-1}$, [Cl$^-$] = 1000 mg dm$^{-3}$; (○●) $i = 100$ A m$^{-2}$, $A/V = 6.5$ m$^{-1}$, [Cl$^-$] = 1000 mg dm$^{-3}$.

**Table 1. Values of the Parameters Used for the Calculation of the Curves in Figure 2**

| run | $A/V$, m$^{-1}$ | $i$, A m$^{-2}$ | $k_m$, m s$^{-1}$ | [Cl$^-$], g dm$^{-3}$ | $\epsilon_F$ |
|---|---|---|---|---|---|
| 1 | 3.3 | 0.2 | $0.98 \times 10^{-5}$ | 1.0 | 0.12 |
| 2 | 3.3 | 0.2 | $0.97 \times 10^{-6}$ | 1.0 | 0.15 |
| 3 | 3.3 | 0.2 | $0.98 \times 10^{-5}$ | 0 | 0.02 |
| 4 | 5.6 | 0.6 | $0.98 \times 10^{-5}$ | 1.0 | 0.28 |
| 5 | 5.6 | 0.3 | $0.98 \times 10^{-5}$ | 1.0 | 0.18 |
| 6 | 6.5 | 1 | $0.97 \times 10^{-6}$ | 1.0 | 0.35 |
| 7 | 6.5 | 0.5 | $0.97 \times 10^{-6}$ | 1.0 | 0.28 |

is plotted versus the specific electric charge supplied per initial mole of phenol ($q_s$). As can be observed, the complete removal of PHB generally requires a greater amount of specific charge with respect to that which is necessary for DCP removal. Moreover, the percentage of PHB removed is more sensitive to a variation of the

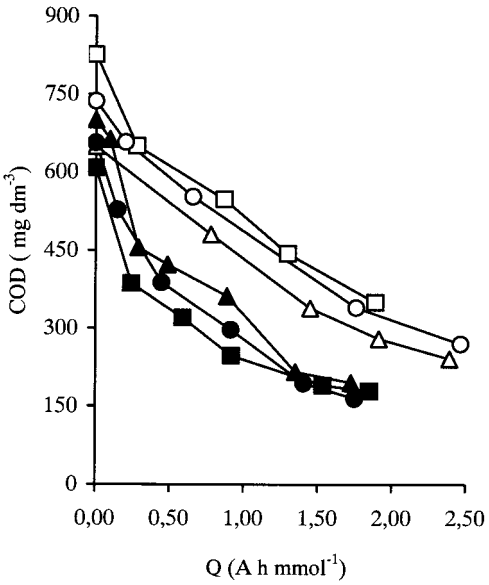


**Figure 5.** Trend of COD during electrochemical oxidation of DCP (full symbols) or PHB (empty symbols) as a function of the specific charge supplied: (△▲) $i = 200$ A m$^{-2}$, $A/V = 6.5$ m$^{-1}$, [Cl$^-$] = 1000 mg dm$^{-3}$, $k_m = 0.97 \times 10^{-6}$ m s$^{-1}$; (□■) $i = 100$ A m$^{-2}$, $A/V = 6.5$ m$^{-1}$, [Cl$^-$] = 1000 mg dm$^{-3}$, $k_m = 0.97 \times 10^{-6}$ m s$^{-1}$; (○●) $i = 20$ A m$^{-2}$, $A/V = 6.5$ m$^{-1}$, [Cl$^-$] = 1000 mg dm$^{-3}$, $k_m = 0.98 \times 10^{-5}$ m s$^{-1}$.

operating conditions. However, in both cases the best results were obtained in the presence of Cl$^-$ by adopting the higher area of anode per unit volume of fluid treated and the lower mass-transfer velocity.

The oxidation process was followed by measurement of the COD of the solution: the trend of COD as a function of $q_s$ is shown in Figure 5. As can be seen, COD initially decreases as the residual phenol concentration decreases as well: at the end of the treatment, when the phenolic compounds have been removed from the solution, the COD value is only 20% of the initial one.

The behavior of COD agrees with the results of the HPLC analysis, which showed, in the initial stage of the process, small amounts of cyclic reaction intermediates, consisting of quinones. In the case of PHB, a larger quantity of these byproducts and traces of chlorinated phenols were detected. For both reactants, a mixture of aliphatic acids with low molecular weight, which may explain the COD value at the end of the process, was observed.

The presence of a not very large amount of chlorinated compounds in the solution agrees with the result previously obtained for phenol oxidation in the presence of NaCl at the Ti/$IrO_2$ anode during which the absence of chlorinated phenol was ascertained. The situation was completely different for the chemical oxidation of phenol with NaClO; here 2-chlorophenol, 2,4-dichlorophenol, and 2,4,6-trichlorophenol were the principal reaction products.[22]

## Discussion

The direct anodic oxidation of organic compounds at the electrode surface with simultaneous oxygen evolution has been widely studied.[25] A comprehensive model[3] for organic oxidation and oxygen evolution has been formulated in which the initial step is the discharge of water molecules to form adsorbed hydroxyl radicals (OH$^\bullet$). Two limiting cases can be distinguished depending on the anodic material: at nonactive electrodes

(boron-doped-diamond or fully oxidized metal oxides such as $SnO_2$ or $PbO_2$) oxidation of organic compounds is an electrochemical step mediated by physisorbed ($OH^•$) radicals from which oxygen can also be produced.

If at the electrode surface oxidizable oxides such as $IrO_2$ or $RuO_2$ are present (active electrodes), the surface itself can be oxidized by limiting the accumulation of $OH^•$: in this case oxidation of organic compounds is a heterogeneous catalytic reaction at electrooxidized active sites, and the release of oxygen occurs in a chemical decomposition step.

The oxidation of organic compounds at active electrodes is slow and not complete. The causes of the improved efficiency of active electrodes for organic oxidative degradation in the presence of $Cl^-$ ions are still not clear.[21] In fact, the hypothesis that chlorohydroxyl radicals are formed during the discharge of chloride does not appear to be able to account for the experimental data.

Also the obvious idea that the degradation takes place by means of electrogenerated $HClO/ClO^-$ does not meet the experimental finding because of the different distribution of byproducts observed in the electrochemical treatment at an active anode in the presence of $Cl^-$ and in the chemical oxidation with NaClO.

To interpret the results obtained in this work for the oxidative degradation of phenols, in the presence of NaCl, that take place at the $RuO_2$ anode simultaneously with oxygen evolution ($E_a \approx 1.3$ vs SCE), we suppose that organic oxidation occurs by combining the heterogeneous reaction at the electrode surface and the homogeneous reaction in the liquid phase;[26] similar hypotheses have been formulated for analogous systems in other works.[27]

In the proposed mechanism, we supposed that the degradation occurs by means of two sequential steps: the first causes the formation of cyclic intermediates (Ic); the second consists of a further oxidation of these byproducts until the cyclic compounds are completely oxidized to aliphatic acid (P), which slowly reacts in the experimental conditions adopted in this work.

The oxidation at the electrode surface occurs by means of the higher metal oxide (MO) and chlorohydroxyl radicals ($R^•$) electrogenerated

$$\mathrm{Ph} \xrightarrow{\mathrm{R^*,\ MO}} \mathrm{Ic} \xrightarrow{\mathrm{R^*,\ MO}} \mathrm{P} \tag{4}$$

The parasitic reaction of $O_2$ evolution can be accomplished by MO decomposition. The radicals can be decomposed to other oxidants (OX) that diffuse from the anode, continuing the oxidation process into the solution.

$$\mathrm{Ph} \xrightarrow{\mathrm{ox}} \mathrm{Ic} \xrightarrow{\mathrm{ox}} \mathrm{P} \tag{5}$$

On the basis of this mechanism, a mathematical model was formulated, that interprets the trend of the concentration of the species involved in the electrolysis at different experimental conditions.

The rate of the electrode reaction (4) can be expressed by pseudo-first-order kinetics with respect to the organic compound concentration ($C_i^s$) at the outer Helmholtz layer.

$$r_i^s = k_i^s C_i^s \tag{6}$$

where $k_i^s$ represents the apparent kinetic constant, which is a function of the current density and which takes into account the coverage degree of oxidizing radicals at the electrode surface.

A second-order kinetics has be adopted to describe the redox reaction in the liquid phase, which can occur both in the diffusion film near the anode surface, whose thickness depends on the hydrodynamic conditions of the reactor, and in the bulk of the solution.

$$r_{i,1} = k_{i,1} C_{\mathrm{Ph}_i} (C_{\mathrm{OX}} - C_{\mathrm{OX}}^*) \tag{7}$$

$$r_{i,2} = k_{i,2} C_{\mathrm{Ic}_i} (C_{\mathrm{OX}} - C_{\mathrm{OX}}^*) \tag{8}$$

In the previous equations, $C_{\mathrm{OX}}^*$ is the minimum OX concentration that gives the half-reaction a sufficiently high potential to oxidize the organic compounds.

Owing to the low reaction rate and the high values of the mass-transfer rate in the cell, the concentration of the organic compounds was assumed to be uniform throughout the reactor.

The OX concentration in the liquid anode film can be obtained from the mole balance equation

$$\frac{\partial C_{\mathrm{OX}}}{\partial t} = D_{\mathrm{OX}} \frac{\partial^2 C_{\mathrm{OX}}}{\partial x^2} - \sum_i \nu_{i,1} r_{i,1} - \sum_i \nu_{i,2} r_{i,2} \tag{9}$$

in which $\nu_{i,1}$ and $\nu_{i,2}$ represent the stoichiometric coefficients of OX in oxidation of organic substrate and intermediates, respectively, $x$ is the distance from the anode surface, and $D_{\mathrm{OX}}$ is the diffusivity of OX ($D_{\mathrm{OX}} = 7 \times 10^{-9}$ m$^2$ s$^{-1}$ [28]). Equation 9 may be simplified, as usual for slow reactions,[29] by uncoupling the time and space integration to obtain the concentration profile of the OX species in the diffusion film near the anode surface at each electrolysis time (see the appendix).

In the bulk liquid phase, the mass balance for OX can be written as

$$\frac{\mathrm{d}C_{\mathrm{OX}}{}^{\mathrm{b}}}{\mathrm{d}t} = \frac{A_a}{V} k_m (C_{\mathrm{OX}}{}^{\mathrm{s}} - C_{\mathrm{OX}}{}^{\mathrm{b}}) - \sum_i \nu_{i,1} r_{i,1} + \sum_i \nu_{i,2} r_{i,2} - \frac{A_c}{V} k_m C_{\mathrm{OX}}{}^{\mathrm{b}} \tag{10}$$

In the previous equation, the following contributions are considered: OX diffusion from the anode surface to the bulk of the solution, reactions between OX and organic substrate in the bulk of the solution, and cathodic reduction of OX (assuming the concentration at the cathode surface to be zero).

As far as the organic compounds (i.e., phenols and further oxidizable reaction intermediates) are concerned, the molar balances can be expressed as

$$\frac{\mathrm{d}n_{\mathrm{Ic}_i}}{\mathrm{d}t} = A_a (r_{i,1}{}^{\mathrm{s}} - r_{i,2}{}^{\mathrm{s}} + \delta (r_{i,1} - r_{i,2})_{\mathrm{film}}) + A_a (L - 2\delta)(r_{i,1} - r_{i,2})_{\mathrm{b}} \tag{11}$$

$$\frac{\mathrm{d}n_{\mathrm{Ph}_i}}{\mathrm{d}t} = -A_a (r_{i,1}{}^{\mathrm{s}} + \delta r_{i,1}|_{\mathrm{film}}) - A_a (L - 2\delta) r_{i,1}|_{\mathrm{b}} \tag{12}$$

In these equations the first term on the right side represents the decrease in the mole number of organic compounds due to reaction at the electrode surface or

**Table 2. Values of the Kinetic Constants in Equations 9−11**

| $i$ | PHB | DCP |
|---|---|---|
| $k_{i,1}$ ($m^3$ $mol^{-1}$ $s^{-1}$) | $5.5 \times 10^{-4}$ | $6 \times 10^{-4}$ |
| $k_{i,2}$ ($m^3$ $mol^{-1}$ $s^{-1}$) | $3 \times 10^{-3}$ | $1 \times 10^{-2}$ |
| $k^s$ (m $s^{-1}$)[a] | $1.5 \times 10^{-7}$ | $2.5 \times 10^{-5}$ |
| $k^s$ (m $s^{-1}$)[b] | $1.2 \times 10^{-8}$ | $3.1 \times 10^{-6}$ |

[a] Solution containing 1 g $dm^{-3}$ of chloride ions. [b] Solution without chloride ions.

in the anode film, while the second accounts for the consumption by reaction in the bulk liquid phase; owing to the low value of the OX concentration in the diffusion film near the cathode surface, the reaction in this volume was neglected.

When the mole balance equations (9)−(12) and the kinetic equations (6)−(8) are combined, a set of $2n + 1$ differential equations can be obtained, in which $n$ is the number of phenolic compounds originally in solution: calculation details can be found in the appendix. The set of equations was integrated by a fourth-order Runge−Kutta numerical method to obtain the trend in time of the organic compounds and the oxidizing species during the electrolysis.

The $k_m$ and $\epsilon_F$ values that were needed for the calculations are reported in Table 1 for the relevant experimental conditions, while the reaction rate constants $k_{i,1}^s$, $k_{i,2}^s$, $k_{i,1}$, and $k_{1,2}$ were found by a trial-and-error procedure and the differences between predicted concentrations and experimental values were used as the criterion for the convergence of iteration. Table 2 shows the kinetic constant values obtained for the two organics investigated. As can be seen, PHB exhibits lower kinetic constants than DCP does; moreover, for both compounds $k_1$ values are lower than $k_2$ values, indicating that, in the adopted conditions, the first reaction step is slower than the second, which involves the opening of the aromatic ring. The higher $k^s$ values in the presence of chlorides can be explained by considering the improved catalytic activity of the surface due to the presence of chlorohydroxyl radicals adsorbed at the active sites of the anode surface.[16]

Figures 6 and 7 show a comparison between experimental and calculated concentrations of phenolic compound, intermediate products, and oxidizing agents, during electrolyses of monocomponent solutions containing 1 g $dm^{-3}$ of chlorides at different electrolyte flow rates. A good agreement between experimental and model-predicted data can be observed, except at longer electrolysis times. The model also allows us to predict the electrolysis time at which the maximum concentration of intermediates from PHB oxidation is achieved. The difference, observed at the end of the process, between the experimental OX concentration and that calculated by the model may be attributed to the consumption of OX by the slow oxidation of the aliphatic products P, a factor not considered by the model.

The formulated model also allows us to explain the great negative effect exerted by an increase in the mass-transfer coefficient during the degradation of PHB. In fact, as is shown in Figure 8 in which the removal percentage in the film is plotted as a function of the global removal, in the case of DCP, because the value of the reaction rate is higher than the diffusion rate of OX from the anode surface to the bulk of the solution, most of the oxidation process is accomplished in the diffusion film near the anode surface even at the maximum flow rate examined. In the case of PHB,

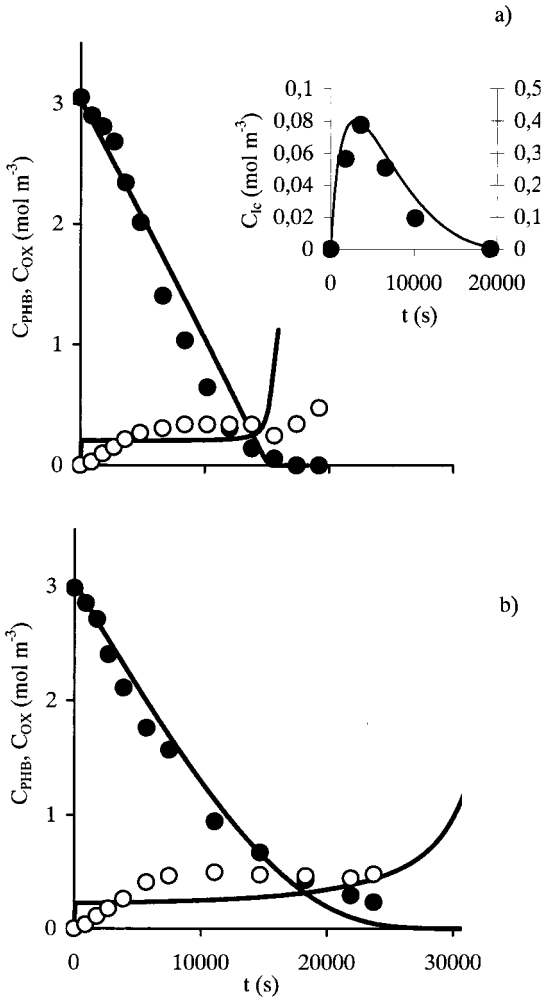


**Figure 6.** Comparison between calculated (lines) and experimental data of PHB (full symbols) and OX (empty symbols) concentrations as a function of time during electrolyses at $i = 200$ A $m^{-2}$ and $A/V = 6.5$ $m^{-1}$: (a) $k_m = 0.97 \times 10^{-6}$ m $s^{-1}$; (b) $k_m = 0.98 \times 10^{-5}$ m $s^{-1}$.

oxidation is confined to the diffusion film only at a lower flow rate: as the flow velocity is increased, the reaction mainly occurs in the bulk of the solution, where the OX concentration becomes lower as the mass-transfer coefficient becomes higher because the reduction of OX at the cathode surface, limited by the mass transfer, becomes important (eq 10).

As far as the effect of the current density is concerned, the specific charge calculated by the model to remove most of the organic compounds decreases by an average of 15% as the current density increases by 50%, according to the results of the experimental runs (see Figures 3 and 4). This behavior may be due to the higher current efficiency values for the production of oxidants observed when higher current density values were imposed.

Figure 9 shows a comparison between experimental and model-predicted data for electrolysis of solutions in which both compounds were present; also in this case, the model matches the experimental values. For both compounds, the effects of the operating parameters on the process agree with those observed during the oxidation of solutions containing only one component. It may also be noted that, if the values of the adopted current density are high enough, the time necessary for the treatment of the solution containing both compounds is the same as that required for the oxidation

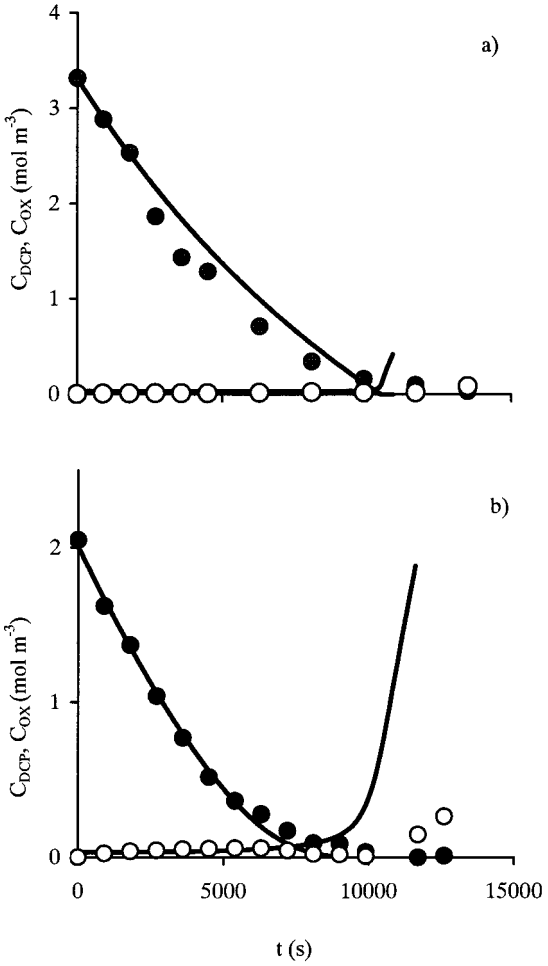


**Figure 7.** Comparison between calculated (lines) and experimental data of DCP (full symbols) and OX (empty symbols) concentrations as a function of time during electrolyses at $i = 200$ A m$^{-2}$ and $A/V = 6.5$ m$^{-1}$: (a) $k_m = 0.97 \times 10^{-6}$ m s$^{-1}$; (b) $k_m = 0.98 \times 10^{-5}$ m s$^{-1}$.

of solutions containing only the less reactive compound. This behavior may be related to better utilization of the oxidant produced at the anode surface when organic compounds with different reactivities are simultaneously present in the solution.

## Conclusions

The results of the present work explain the complex effect of the operating parameters on the electrochemical degradation of the examined compounds, which are similar to those previously observed during the electrochemical treatment of real wastewaters.[30] In particular, the formulated model takes into account the synergetic effect of both direct oxidation by electrogenerated radicals sorbed on the active sites at the electrode surface and indirect oxidation by oxidants that are produced from the destruction of the radicals themselves. These oxidants have a long life and may spread to the bulk of the solution, continuing the oxidation process. These mechanisms occur to various extents depending on the reactivity of the organic substrate and are differently affected by the operating conditions. The direct reaction mechanism is favored by high values of both current density and mass-transfer coefficients, while the indirect reaction mechanism is hindered by high values of $k_m$ when an undivided cell is used, owing

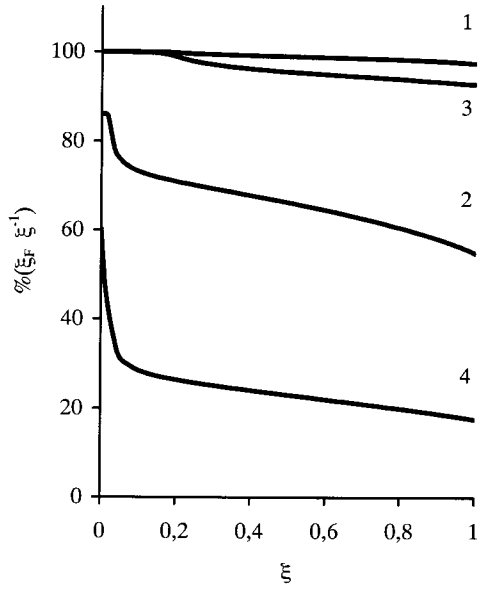


**Figure 8.** Percentage of removal of DCP (full lines) or PHB (dotted lines) achieved in the anode film as a function of the total removal of each organic compound. The data were calculated at $i = 200$ A m$^{-2}$ and $A/V = 6.5$ m$^{-1}$ by using $k_m = 0.97 \times 10^{-6}$ m s$^{-1}$ (1 and 3) or $k_m = 0.98 \times 10^{-5}$ m s$^{-1}$ (2 and 4).

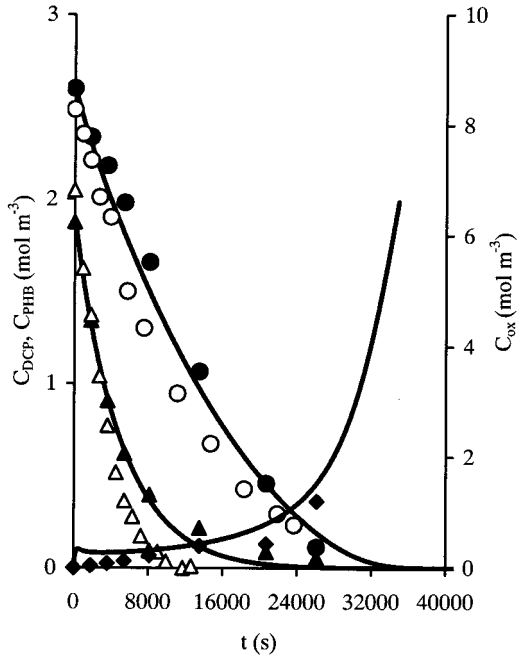


**Figure 9.** Comparison between calculated (lines) and experimental data of PHB (○●), DCP (△▲), and OX (◆) concentrations as a function of time during electrolyses of solutions containing one (empty symbols) or both components (full symbols) at $i = 200$ A m$^{-2}$, $k_m = 0.98 \times 10^{-5}$ m s$^{-1}$, and $A/V = 6.5$ m$^{-1}$.

to the faster consumption of the soluble oxidants at the cathode surface.

The results show that the mathematical model presented in this paper may constitute a useful tool to select the operative conditions for an electrochemical reactor, on the basis of the chemical composition of the wastewater to be treated and the adopted anode material.

## Appendix

To obtain the concentration profile of the oxidizing species in the diffusion film near the anode surface, the following hypotheses were assumed:

(i) Pseudo-steady-state conditions for the concentration of the oxidizing agent in the diffusion layer.

$$\frac{\partial C_{OX}}{\partial t} \cong 0 \tag{A1}$$

(ii) Uniform concentration of the organic compounds throughout the reactor.

$$\frac{\partial C_{Ph_i}}{\partial x} \cong 0 \qquad \frac{\partial C_{Ic_i}}{\partial x} \cong 0 \tag{A2}$$

Therefore, eq 9 can be written as

$$\frac{d^2 C_{OX}}{dx^2} = \beta (C_{OX} - C^*_{OX}) \tag{A3}$$

where

$$\beta = \left[ \frac{\sum_i \nu_{i,1} k_{i,1} C_{Ph_i} + \sum_i \nu_{i,2} k_{i,2} C_{Ic_i}}{D_{OX}} \right] \tag{A4}$$

is only time-dependent.

Integrating eq A3 with the boundary conditions

$$x = 0 \qquad \frac{dC_{OX}}{dx} = -\epsilon_F \frac{i}{zFD_{OX}} \tag{A5}$$

$$x = \delta \qquad C_{OX} = C_{OX}{}^b$$

we obtain

$$C_{OX}(x,t) - C^*_{OX} = (C_{OX}{}^b - C^*_{OX}) \frac{e^{-\sqrt{\beta}x} + e^{\sqrt{\beta}x}}{e^{-\sqrt{\beta}\partial} + e^{\sqrt{\beta}\partial}} + \epsilon_F \frac{i}{zFD_{OX}\sqrt{\beta}} \frac{e^{\sqrt{\beta}(\partial - x)} - e^{-\sqrt{\beta}(\partial - x)}}{e^{-\sqrt{\beta}\partial} + e^{\sqrt{\beta}\partial}} \tag{A6}$$

By substituting in eq 10 the kinetic eqs 7 and 8 and the value of $C_{OX}{}^s$ calculated by eq A6 at $x = 0$, we obtain

$$\frac{dC_{OX}{}^b}{dt} = \frac{A_a}{V} k_m \left( (C_{OX}{}^b - C^*_{OX}) \frac{2}{e^{-\sqrt{\beta}\partial} + e^{\sqrt{\beta}\partial}} + \epsilon_F \frac{i}{zFD_{OX}\sqrt{\beta}} \frac{e^{\sqrt{\beta}\partial} - e^{-\sqrt{\beta}\partial}}{e^{-\sqrt{\beta}\partial} + e^{\sqrt{\beta}\partial}} - C^*_{OX} - C_{OX}{}^b \right) - (C_{OX}{}^b - C^*_{OX}) \left( \sum_i \nu_{i,1} k_{i,1} C_{Ph_i} + \sum_i \nu_{i,2} k_{i,2} C_{Ic_i} \right) - \frac{A_c}{V} k_m C_{OX}{}^b \tag{A7}$$

As far as the organic compounds are concerned, on the basis of the hypotheses (A2) and with the reaction rates expressed by eqs 6−8, the following equations can be obtained:

$$\frac{dC_{Ph_i}}{dt} = -\frac{A_a}{V} (k_i{}^s C_{Ph_i} - \delta r_{i,1}|_{film}) - \frac{A_a}{V} (L - 2\delta) k_{i,1} C_{Ph_i} (C_{OX}{}^b - C^*_{OX}) \tag{A8}$$

$$\frac{dC_{Ic_i}}{dt} = \frac{A_a}{V} (k_i{}^s C_{Ph_i} - k_i{}^s C_{Ic_i} + \delta (r_{i,1} - r_{i,2})|_{film}) + \frac{A_a}{V} (L - 2\delta)(k_{i,1} C_{Ph_i} - k_{i,2} C_{Ic_i})(C_{OX}{}^b - C^*_{OX}) \tag{A9}$$

The reaction rate in the diffusion layer has been expressed by means of its average value in the range of $x$ between 0 and $\delta$:

$$r_{i,1}|_{film} = \frac{1}{V_f} \int_0^{V_f} k_{i,1} C_{Ph_i} (C_{OX} - C^*_{OX})\, dV = \frac{1}{\delta} \int_0^{\delta} k_{i,1} C_{Ph_i} (C_{OX} - C^*_{OX})\, dx \tag{A10}$$

$$r_{i,2}|_{film} = \frac{1}{V_f} \int_0^{V_f} k_{i,2} C_{Ic_i} (C_{OX} - C^*_{OX})\, dV = \frac{1}{\delta} \int_0^{\delta} k_{i,2} C_{Ic_i} (C_{OX} - C^*_{OX})\, dx \tag{A11}$$

Substituting eq A6 into eqs A10 and A11 and integrating, we obtain

$$r_{i,1}|_{film} = \frac{1}{\delta} k_{i,1} C_{Ph_i} \left[ \frac{(C_{OX}{}^b - C^*_{OX})}{\sqrt{\beta}} \frac{e^{\sqrt{\beta}\partial} - e^{-\sqrt{\beta}\partial}}{e^{-\sqrt{\beta}\partial} + e^{\sqrt{\beta}\partial}} + \epsilon_F \frac{i}{zFD_{OX}\beta} \frac{e^{\sqrt{\beta}\partial} + e^{-\sqrt{\beta}\partial} - 2}{e^{-\sqrt{\beta}\partial} + e^{\sqrt{\beta}\partial}} \right] \tag{A12}$$

$$r_{i,2}|_{film} = \frac{1}{\delta} k_{i,2} C_{Ic_i} \left[ \frac{(C_{OX}{}^b - C^*_{OX})}{\sqrt{\beta}} \frac{e^{\sqrt{\beta}\partial} - e^{-\sqrt{\beta}\partial}}{e^{-\sqrt{\beta}\partial} + e^{\sqrt{\beta}\partial}} + \epsilon_F \frac{i}{zFD_{OX}\beta} \frac{e^{\sqrt{\beta}\partial} + e^{-\sqrt{\beta}\partial} - 2}{e^{-\sqrt{\beta}\partial} + e^{\sqrt{\beta}\partial}} \right] \tag{A13}$$

In eq A7 and eqs A8 and A9, in which the value of $r|_{film}$ is expressed by eqs A13 and A14, we obtain a set of $2n + 1$ differential equations, in which $n$ is the number of phenols originally in the solution.

## List of Symbols

$A$ = area, $m^2$
$C$ = concentration, mol $m^{-3}$
$D$ = diffusion coefficient, $m^2$ $s^{-1}$
$F$ = Faraday's constant, C $mol^{-1}$
$I$ = current intensity, A
$i$ = current density, A $m^{-2}$
$Q$ = electrolyte flow rate, $m^3$ $s^{-1}$
$t$ = times
$k_s$ = first-order kinetic constant, m $s^{-1}$
$k$ = second-order kinetic constant, $m^3$ $mol^{-1}$ $s^{-1}$
$k_m$ = mass-transfer coefficient, m $s^{-1}$
$r_s$ = reaction rate, mol $m^{-2}$ $s^{-1}$
$r$ = reaction rate, mol $m^{-3}$ $s^{-1}$
$u$ = electrolyte linear velocity, m $s^{-1}$
$V$ = electrolyte volume, $m^3$
$z$ = number of electrons

*Greek Symbols*

$\epsilon_F$ = faradaic yield
$\xi$ = percentage of pollutant removal
$\delta$ = thickness of liquid film, m
$\nu$ = stoichiometric coefficient

*Superscripts*

b = bulk
s = surface

*Subscripts*

a = anode
c = cathode
OX = oxidizing species

## Literature Cited

(1) Rajeshwar, K.; Ibnez, J. *Fundamentals and applications in pollution abatement*; Academic Press: New York, 1997.

(2) Polcaro, A. M.; Palmas, S. Electrochemical Oxidation of Chlorophenols. *Ind. Eng. Chem. Res.* **1997**, *36*, 1791.

(3) Simond, O.; Schaller, V.; Comninellis, C. Theoretical Model for the Anodic Oxidation of Organics on Metal Oxide Electrodes. *Electrochim. Acta* **1997**, *42* (13−14), 2009−2012.

(4) Gattrell, M.; Kirk, W. A Study of the oxidation of phenol at platinum and preoxidised platinum surfaces *J. Electrochem. Soc.* **1993**, *140* (6), 1534.

(5) Wu, Z. C.; Zhou, M. H. Partial degradation of phenol by advanced electrochemical oxidation process. *Environ. Sci. Technol.* **2001**, *35* (13), 2698.

(6) Rodgers, J. D.; Jedral, W.; Bunce, N. J. Electrochemical oxidation of chlorinated phenols. *Environ. Sci. Technol.* **1999**, *33*, 1453.

(7) Johnson, S. K.; Houk, L. L.; Feng, J. R.; Houk, R. S.; Johnson, D. C. Electrochemical incineration of 4-chlorophenol and the identification of products and intermediates by mass spectrometry. *Environ. Sci. Technol.* **1999**, *33*, 2638−2644.

(8) Stucki, S.; Kotz, R.; Carcer, B.; Suter, W. Electrochemical wastewater treatment using high overvoltage anodes. Part II. *J. Appl. Electrochem.* **1991**, *21*, 99.

(9) Comninellis, C.; Pulgarin, C. Electrochemical oxidation of phenol for wastewater treatment using $SnO_2$ Anodes. *J. Appl. Electrochem.* **1993**, *23*, 108.

(10) Feng, J. R.; Houk, L. L.; Johnson, D. C.; Lowery, S. N.; Carey, J. J. Electrocatalysis of Anodic Oxygen-Transfer Reactions—The Electrochemical Incineration of Benzoquinone. *J. Electrochem. Soc.* **1995**, *142*, 3626−3632.

(11) Beck, F.; Krohn, H.; Kaiser, W.; Fryda, M.; Klages, C. P.; Schafer, L. Boron Doped Diamond/Titanium Composite Electrodes for Electrochemical Gas Generation from Aqueous Electrolytes. *Electrochim. Acta* **1998**, *44*, 525−532.

(12) Rodrigo, M. A.; Michaud, P. A.; Duo, I.; Panizza, M.; Cerisola, G.; Comninellis, C. Oxidation of 4-chlorophenol at boron-doped diamond electrode for wastewater treatment. *J. Electrochem. Soc.* **2001**, *148*, D60.

(13) Szpyrkowicz, L.; Kelsall, G. H.; Kaul, S. N.; De Faveri, M. Performance of electrochemical reactor for treatment of tannery wastewaters. *Chem. Eng. Sci.* **2001**, *56*, 1579.

(14) Cossu, R.; Polcaro, A. M.; Lavagnolo, M. C.; Mascia, M.; Palmas, S.; Renoldi, F. Electrochemical Treatment of Landfill Leachate—Oxidation at $Ti/PbO_2$ and $Ti/SnO_2$ Anodes. *Environ. Sci. Technol.* **1998**, *32*, 1270.

(15) Naumczyk, J.; Szpyrkowicz, L.; Ziliograndi, F. Electrochemical Treatment of Textile Wastewater. *Water Sci. Technol.* **1996**, *34*, 17.

(16) Israilides, C. J.; Vlyssides, A. G.; Mourafeti, V. N.; Karvouni, G. Olive Oil Wastewater Treatment with the Use of an Electrolysis System. *Bioresour. Technol.* **1997**, *61*, 163.

(17) Chiang, L. C.; Chang, J. E.; Wen, T. C. Indirect Oxidation Effect in Electrochemical Oxidation Treatment of Landfill Leachate. *Water Res.* **1995**, *29*, 671.

(18) Comninellis, C.; Pulgarin, C. Anodic oxidation of phenol for wastewater treatment. *J. Appl. Electrochem.* **1991**, *21*, 703.

(19) Gattrell, M.; MacDougall, B. The anodic electrochemistry of pentachlorophenol. *J. Electrochem. Soc.* **1999**, *146*, 3335−3348.

(20) Bonfatti, F.; De Battisti, A.; Ferro, S.; Lodi, G.; Osti, S. Anodic mineralization of organic substrates in chloride-containing aqueous media. *Electrochim. Acta* **2000**, *46*, 305−314.

(21) Bonfatti, F.; Ferro, S.; Lavezzo; F.; Malacarne, M.; Lodi, G.; De Battisti, A. Electrochemical incineration of glucose as a model organic substrate—II. Role of active chlorine mediation. *J. Electrochem. Soc.* **2000**, *147*, 592−596.

(22) Comninellis, C.; Nerini, A. Anodic Oxidation of Phenol in the Presence of Nacl for Wastewater Treatment. *J. Appl. Electrochem.* **1995**, *25*, 23.

(23) Greef, R.; Peat, R.; Peter, L. M.; Pletcher, D.; Robinson, J. *Instrumental Methods in Electrochemistry*; Ellis Horwood: Chichester, U.K., 1985; p 113.

(24) Perry, R.; Green, D. *Chemical Engineers' Handbook*; McGraw-Hill: New York, 1997; pp 5−59.

(25) Rajeshwar, K.; Ibanez, J. *Environmental Electrochemistry*: *Fundamental and Applications in Pollution Abatement*; Academic Press: New York, 1997; p 363.

(26) Polcaro, A. M.; Palmas, S.; Lallai, A. Sequential electrochemical/biological treatment for the removal of 2,6-dichlorophenol from synthetic wastewater. *Ann. Chim. (Rome)* **2001**, *91*, 203−210.

(27) Saracco, G.; Solarino, L.; Specchia, V.; Maja, M. Electrolytic abatement of biorefractory organics by combining bulk and electrode oxidation processes. *Chem. Eng. Sci.* **2001**, *56*, 1571.

(28) Perry, R.; Green, D. *Chemical Engineers' Handbook*; McGraw-Hill: New York, 1997; pp 5−50.

(29) Trambouze, P.; Van Landghem, H.; Wauquier, J. P. *Chemical Reactors*; Editions Technip: Paris, 1998; p 237.

(30) Szpyrkowicz, L.; Zilio-Grandi, F.; Kaul, S. N.; Polcaro, A. M. Copper electrodeposition and oxidation of complex cyanide from wastewater in an electrochemical reactor with a Ti/Pt anode. *Ind. Eng. Chem. Res.* **2000**, *39*, 2132.

*Received for review* August 8, 2001
*Revised manuscript received* February 22, 2002
*Accepted* March 28, 2002

IE010669U